Available online at www.sciencedirect.com
ScienceDirect
Journal of Sound and Vibration 317 (2008) 50–66
JOURNAL OF SOUND AND VIBRATION
www.elsevier.com/locate/jsvi

An investigation of an active landing gear system to reduce aircraft vibrations caused by landing impacts and runway excitations

Haitao Wang[a,b], J.T. Xing[a,*], W.G. Price[a], Weiji Li[b]

[a]*School of Engineering Sciences, Ship Science, University of Southampton, Highfield, Southampton SO17 1BJ, UK*
[b]*School of Aeronautics, Northwestern Polytechnical University, Xi'an 710072, People's Republic of China*

Received 20 June 2007; received in revised form 4 March 2008; accepted 12 March 2008
Handling Editor: M.P. Cartmell
Available online 12 May 2008

Abstract

A mathematical model is developed to control aircraft vibrations caused by runway excitation using an active landing gear system. Equations are derived to describe the integrated aircraft-active system. The nonlinear characteristics of the system are modelled and it is actively controlled using a Proportional Integral Derivative (PID) strategy. The performance of this system and its corresponding passive system are compared using numerical simulations. It is demonstrated that the impact loads and the vertical displacement of the aircraft's centre of gravity caused by landing and runway excitations are greatly reduced using the active system, which result in improvements to the performance of the landing gear system, benefits the aircraft's fatigue life, taxiing performance, crew/passenger comfort and reduces requirements on the unevenness of runways.

1. Introduction

An aircraft landing gear system must absorb the kinetic energy produced by a landing impact and excitations caused by the aircraft travelling over an uneven runway surface. This is the necessary requirement of a successfully designed landing system [1,2].

The oleo-pneumatic shock strut shown in Fig. 1 and described in principle in Section 2 is the most common type of shock absorber landing gear system used in aircrafts. It dissipates the kinetic energy produced by impacts arising when an airplane lands at high speed but also offers a comfortable ride to passengers when the airplane taxies at low speed. The strut behaves in a strongly nonlinear manner, which influences the performance of the landing system [3–5]. Investigations [6–9] involving real-time feedback of the ground input to the landing system have shown that active control greatly reduces impact and fatigue loads experienced by the aircraft as well as vertical displacements. This is achieved by adjusting the system's stiffness and damping

*Corresponding author. Tel.: +44 2380596549; fax: +44 2380593299.
E-mail address: jtxing@soton.ac.uk (J.T. Xing).

0022-460X/$ - see front matter © 2008 Elsevier Ltd. All rights reserved.
doi:10.1016/j.jsv.2008.03.016

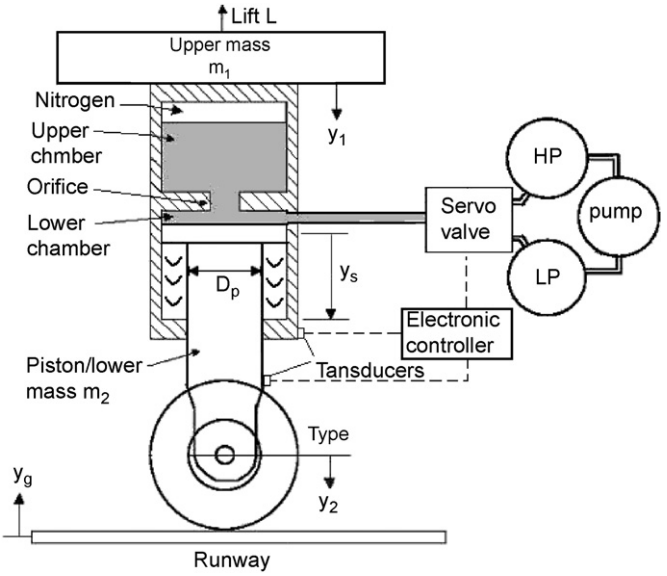

Fig. 1. A model of an active landing gear system with an active control system. HP denotes a high-pressure accumulator and LP represents a low-pressure reservoir. The passive system does not include the servo valve, etc. components.

values [6–9]. In most current airplane designs, a traditional passive landing gear system is used [10]. The impact loads experienced are large [11], because the characteristic design parameters of a shock-absorbing device in a passive system cannot adjust to meet different landing and runway environments. In very bad landing conditions, large impact loads can reach the design limitations of the airframe and landing gear structure to cause a possible flight accident [11,12].

The development of shock absorber control technology is identified by passive, semi-active and active control phases [10]. The major difference between an active and a passive control landing gear system is that the hydraulic fluid flow in the absorber is controlled by ground-induced aircraft vibration loads and therefore the hydraulic damping is changed following the shock strut stroke and the impact load [12]. This improves the performance of the active control shock absorber and the resulting vibration reduced by designing a suitable controller. Through measurement of the strut's stroke, the controller influences a servo valve which regulates the hydraulic fluid flow. This subsequently alters the damping characteristic and hence reduces the vibration [12].

At present, active control landing gear systems are still in the stage of theoretical and experimental investigation. They have not been introduced into real aircrafts because of many practical issues involving safety, design and production. Previously, NASA studied the behaviour of an active nose landing gear using A-10 [6] and F-106B [7] airplanes. In the latter, drop tests were performed. These two studies focussed on observation and experimental data but lacked a theoretical analysis to support the tests. Ghiringhelli [13] tested a semi-active landing gear control system of a generic aircraft, but it was shown that its overall influence was inferior compared to an active controller. This situation contrasts markedly to developments in automotive engineering [14–16] where an active control approach is widely used.

This paper develops a detailed nonlinear mathematical model to describe an active landing gear system. Based on this model, the dynamic equations derived are used to investigate the behaviour of an aircraft-active landing gear interaction system subject to runway excitation. The stability of the integrated system around its static equilibrium position is studied and SIMULINK control system simulation software [17] is used to validate the theoretical analysis. The simulations allow comparison of performance of the active and passive control systems. It is shown that impact load and vertical displacement of the aircraft's centre of gravity are greatly reduced using an active landing gear system. Furthermore, the vibration load is reduced, the influence of unevenness in the runway decreased and improvements are observed in the behaviour of the fatigue life of the fuselage and landing gear, landing gear and taxiing performance, crew and passenger comfort and the

pilot's ability to control the plane during ground operations. The developed model and analysis method provide a fundamental approach to design and investigate active control landing gear systems.

2. Mathematical model of an active control landing gear system

Fig. 1 illustrates a model of an active landing gear system with a typical oleo-pneumatic shock absorber [18,19]. The absorber is the main component of a passive system. It consists of lower and upper chambers of cross-sectional areas A_1 and A_2, respectively. These two chambers are connected by a small orifice of diameter D_{op} [8]. The upper volume of the top chamber is filled with pressurised nitrogen and the remaining volumes of the upper and lower chambers are filled with oil. This absorber design produces both spring and damping characteristics. During the process of an airplane landing, the shock strut experiences compression and extension. This motion forces the oil to pass through the orifice, which dissipates the large amount of energy created by a landing impact. The oil flows from the lower to the upper chamber, compressing the nitrogen that stores the remaining impact energy. When this stored energy is released, the shock strut extends and the oil flows from the upper to the lower chamber, thus dissipating the impact energy residue. This compression and extension oscillation continues until all landing impact energy dissipates.

To this active landing gear system, an active control system is added as shown in Fig. 1. The latter consists of a servo valve, a low-pressure (LP) reservoir, a high-pressure (HP) accumulator, a hydraulic pump, an electronic controller and feedback transducers. When an aircraft lands, the shock absorber stroke is influenced by the aircraft's payload and varies depending on runway excitation. The stroke is measured by the transducers and their signals input into the electronic controller. This directs the servo valve to regulate the oil flow into or out of the shock absorber, hence producing the active control force to reduce the force transferred to the airplane. As will be shown, this action improves the performance of the passive system.

To establish a mathematical model to describe this active landing gear system, the notation adopted is shown in Fig. 2. Here, the airplane and possible attachments (e.g. cylinder, etc.) are simplified by a concentrated mass m_1 to which an aerodynamic lift L is applied. The landing gear's piston of diameter D_p and the plane's tyre are modelled by the lumped mass m_2. These two masses are connected by a spring of stiffness $k_1$and a damper of damping coefficient c_1, which simulate the stiffness and damping of the shock strut unit. The spring of stiffness k_2 and damper of damping coefficient c_2 represent the stiffness and damping of the piston and the airplane's tyre, respectively. The system's reference configuration initial state occurs at the instant when the landing gear is fully extended and the tyre first touches the ground such that the displacements of masses m_1, m_2 and piston are each of zero value, i.e. $y_1 = 0 = y_2 = y_3$. Subsequently, the landing gear system is subject to a ground input displacement represented by y_g.

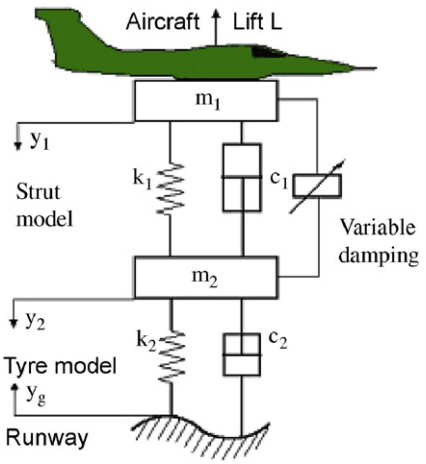

Fig. 2. Schematic illustration of the dynamic model of the active landing gear system shown in Fig. 1.

2.1. Dynamic equilibrium equations

Using Newton's second law of motion and examining the dynamic equilibria of the two masses shown in Fig. 2, we represent the dynamic equations describing the system by

$$m_1\ddot{y}_1 = m_1 g - L - F_a - F_l - f - F_Q, \tag{1}$$

$$m_2\ddot{y}_2 = m_2 g + F_a + F_l - F_t + f + F_Q. \tag{2}$$

Here F_a and $F_l$denote the spring and damping forces of the shock absorber, respectively, F_t the ground supporting force, f the friction force between the piston and the cylinder wall, F_Q the active control force and g the gravitational acceleration constant. These forces involve physical nonlinear mechanisms, which are now discussed.

2.2. Spring force F_a

The spring force F_a simulates the force produced by the pressure of the nitrogen gas in the upper chamber. It is assumed that the pressure p and volume V of this gas satisfy the equations of the state of gases in the form [20]

$$\frac{p_0}{p} = \left(\frac{V}{V_0}\right)^n, \tag{3}$$

$$V = V_0 - Ay_s = A(y_0 - y_s), \tag{4}$$

$$F_a = pA. \tag{5}$$

Here p_0, V_0, y_0, p and V represent the initial gas pressure, volume, length of the gas cylinder, the current gas pressure and volume, respectively, $A = \pi {D_p}^2/4$ denotes the cross-sectional area of the piston, $y_s = y_1 - y_2$ the shock absorber stroke and n is a gas constant of value normally 1.1 [20]. Obviously, $V_0 = Ay_0$, and the initial gas length constant y_0 is used for non-dimensionalisation purposes, i.e. $y_1 - y_2/y_0$. The combination of Eqs. (3–5) yields

$$F_a = p_0 A\left(\frac{V_0}{V}\right)^n = p_0 A\left(\frac{V_0}{V_0 - Ay_s}\right)^n = p_0 A\left(\frac{1}{1-(y_1 - y_2/y_0)}\right)^n. \tag{6}$$

2.3. Damping force F_l

The damping force depends on the energy dissipated by of the oil flowing through the orifice. It is assumed that the oil is incompressible and p_1 represents the difference between the pressures of the lower and upper chambers. From the mass conservation law and Bernoulli's equation [20], the following two equations are derived:

$$A\dot{y}_s = \xi A_0 V_l, \tag{7}$$

$$p_l = \tfrac{1}{2}\rho(V_l^2 - \dot{y}_s^2). \tag{8}$$

The parameter ξ represents an orifice discharge coefficient, which is determined by experiment [20], $A_0 = \pi {D_{op}}^2/4$ denotes the orifice area, V_1 represents the velocity of the oil flowing through the orifice and ρ is the mass density of the oil. Eqs. (7,8) give

$$p_l = \frac{1}{2}\rho\left(\frac{A^2}{\xi^2 A_0^2} - 1\right)\dot{y}_s^2 \approx \frac{1}{2}\rho\frac{A^2}{\xi^2 A_0^2}\dot{y}_s^2 \tag{9}$$

from which the damping force is derived as

$$F_l = p_l A = \frac{1}{2}\rho\frac{A^3\dot{y}_s|\dot{y}_s|}{\xi^2 A_0^2}. \tag{10}$$

Here, $\dot{y}_s^2$ is replaced by $\dot{y}_s|\dot{y}_s|$ to permit the damping force F_l to be positive corresponding to a positive velocity $\dot{y}_s$ as defined in Eqs. (1 and 2). Physically, $\dot{y}_s = \dot{y}_1 - \dot{y}_2$ denotes the velocity of the piston relative to the outside cylinder of the oleo-pneumatic shock absorber. If $\dot{y}_s = 0$, the oil is static and it does not flow through the orifice, giving a zero force F_l.

2.4. Ground reaction force F_t

The force transmitted through the tyre from the ground is governed by the expression [21]

$$F_t = k_t(y_2 + y_g) + c_t(\dot{y}_2 + \dot{y}_g), \tag{11}$$

where a linear tyre characteristic is assumed and therefore the stiffness k_t and damping coefficient c_t are considered as two constants.

2.5. Friction force f

Additional friction forces experienced by the landing gear are generated from two principal sources. Namely, one force F_{seal} is caused by the tightness of the seal and the other friction force F_{ow} is due to the offset wheel [8]. The former is calculated by [8]

$$F_{\text{seal}} = k_m\dot{y}_s + \text{sgn}(\dot{y}_s)k_n\dot{y}_s^2, \tag{12}$$

where k_m and k_n denote two coefficients and $\text{sgn}(\dot{y}_s)$ is defined by

$$\text{sgn}(\dot{y}_s) = \begin{cases} 1, & \dot{y}_s > 0, \\ 0, & \dot{y}_s = 0, \\ -1, & \dot{y}_s < 0. \end{cases} \tag{13}$$

Here, the function $\text{sgn}(\dot{y}_s)$ is artificially introduced in order to use one equation as shown by Eq. (12) to represent the damping force in the negative direction of the relative velocity $\dot{y}_s = \dot{y}_1 - \dot{y}_2$. For this artificial function defined by Eq. (13), $\dot{y}_s = 0$ is a solitary point at which its mathematical derivative does not exist. However, from a physical viewpoint, the real damping force term $\pm k_n\dot{y}_s^2$ vanishes at this point. The curve of this term, as a function of $\dot{y}_s = \dot{y}_1 - \dot{y}_2$, illustrates symmetry relative to the centre of origin of the coordinate system. It is noted that this curve is continuous and differentiable with no jump phenomena exhibited at its centre. If derivative operations are required in the numerical simulation, the three equations expressed in Eq. (13) are used. Therefore, this artificial function with a solitary singular point $\dot{y}_s = 0$ does not cause any simulation difficulty. Furthermore, at point $\dot{y}_s = 0$ we can always impose a zero value of its first derivative with respect to $\dot{y}_s$, to satisfy the physical characteristic of a real damping force.

The mechanism creating the friction force F_{ow} is illustrated and modelled in Fig. 3 in which a normal force N between the piston head and the cylinder wall is caused by the design of the offset wheel [8]. This force is required to balance the tyre force F_t applied at a distance l from the centreline of the piston. The balance equation is given by

$$N(y_s + B) = F_t l, \tag{14}$$

where B is defined as one-half of the thickness of the lower bearing. From this equation, it follows that

$$N = \frac{F_t l}{y_s + B}, \tag{15}$$

so that the frictional force due to the offset wheel can be calculated by

$$F_{ow} = \mu N = \mu\left(\frac{F_t l}{y_s + B}\right), \tag{16}$$

where μ is the coefficient of friction on the interface between the cylinder and the piston.

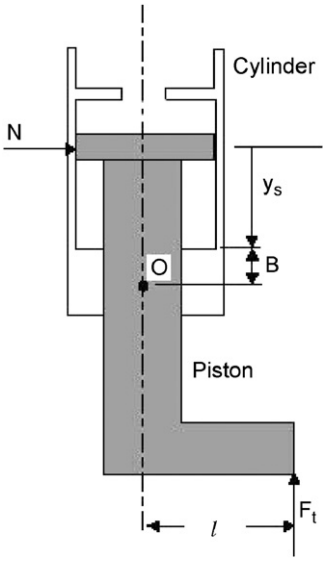

Fig. 3. Landing gear friction force due to offset wheel design.

The total friction force of the landing gear f is given by

$$f = F_{\text{seal}} + F_{ow}. \tag{17}$$

2.6. Active control force F_Q

The active control force F_Q is a function of the flow quantity Q adjusted by the displacement x of the servo valve, which is further controlled by the signal $\dot{y}_1 - \dot{y}_2$ measured by the transducers. Presently, an exact analytical relationship between the active control force F_Q and the flow quantity Q is very difficult to establish. It is often determined through experiments or by empirical formula [12]. From this evidence, it is assumed that the active control force is described by

$$F_Q = k_a Q + k_b Q|Q|, \tag{18}$$

where k_a and k_b are the two characteristic constants measured for a designed servo-valve system [12].

The flow quantity Q is calculated by

$$Q = C_d w x \sqrt{\frac{|p_s - p_l|}{\rho}}. \tag{19}$$

Here p_s is a pressure with $p_s = p_{sh}$, $p_s = p_{s1}$ in the HP and LP reservoirs, respectively, as shown in Fig. 1, C_d represents a non-dimensional discharge coefficient, w defines the gradient of area of the servo-valve port and x represents the displacement of the servo valve. When the servo valve is positively opened, $x>0$ and the oil is drawn from the HP reservoir into the landing gear, producing a positive flow quantity $Q>0$ and a positive active control force $F_Q>0$. On the contrary, when the servo valve is negatively opened ($x<0$), oil is drawn from the landing gear into the LP reservoir so that $Q<0$ and $F_Q<0$.

The displacement x of the servo valve is controlled by Proportional Integral Derivative (PID) control signals [22] as shown in Fig. 4. The PID controller combines system motion information, allowing generation of a synthesised control signal. It has the advantage of being structurally simple, mathematically credible, relatively easy to realise with scope for adjustment, thus making it widely applicable in engineering systems [22]. The PID controller is chosen to complete the mathematical model and to investigate the landing gear system's performance but it is not the intention of this paper to focus on deriving new control laws [23].

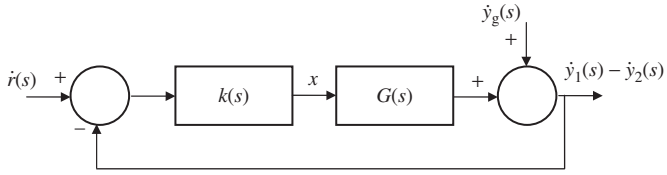

Fig. 4. Schematic sketch of the Proportional Integral Derivative (PID) controller.

In Fig. 4, $\dot{r}(t)$ represents a reference signal and $\dot{y}_1 - \dot{y}_2$ is the feedback signal measured from the landing gear. Their difference

$$e(t) = \dot{r}(t) - (\dot{y}_1 - \dot{y}_2) \tag{20}$$

is input into the PID controller for which the transfer function is defined as [22]

$$k(s) = k_p + \frac{k_i}{s} + k_d s. \tag{21}$$

Here, k_p represents a proportionality coefficient, k_i an integral coefficient and k_d a differential coefficient. These feedback coefficients can be adjusted to obtain the best control efficiency. Since the velocity signal is used as a feedback signal, the integral, proportional and differential coefficients physically represent displacement, velocity and acceleration feedback gains, respectively. The output signal of the controller gives the displacement of the servo valve as [24,25]

$$\begin{aligned} x(t) = {} & k_p\{\dot{r}(t) - [\dot{y}_1(t) - \dot{y}_2(t)]\} + k_i\{r(t) - [y_1(t) - y_2(t)]\} \\ & + k_d\{\ddot{r}(t) - [\ddot{y}_1(t) - \ddot{y}_2(t)]\}. \end{aligned} \tag{22}$$

3. Stability analysis

From the viewpoint of a practical engineering application, we assume that, in time, the aircraft returns to its static equilibrium position after a landing impact or a runway excitation. A passive landing system satisfies this assumption. As shown in Fig. 1, an active landing system is established by the introduction of an active control unit. This unit provides additional damping and stiffness forces to improve the performance of the passive landing gear system. These additional forces play a modifying role with the expectation that they cause the aircraft to return to its static equilibrium position quicker than by the passive gear system only.

As a part of this investigation, we aim to confirm whether the static equilibrium solution of the nonlinear ordinary differential equations governing the motion of the system is asymptotically stable. Based on the theory of ordinary differential equations, the asymptotic stability of the system is deduced by investigating a linearised system [26]. That is, if all eigenvalues of the linearised equation have negative real parts, then the static equilibrium solution of the original nonlinear system is asymptotically stable. This is achieved by examining the sign of the Routh–Hurwitz determinants [27] by (i) determining the static equilibrium solution of the nonlinear system, (ii) establishing a linearised approximate equation describing the dynamic solution relative to the static equilibrium solution, and (iii) checking whether the Routh–Hurwitz determinants are positive.

3.1. Matrix equations

To provide an effective stability analysis, the equations derived in Section 2 are rewritten in the following matrix forms.

Dynamic equilibrium equations

$$\begin{bmatrix} m_1 & 0 \\ 0 & m_2 \end{bmatrix} \begin{bmatrix} \ddot{y}_1 \\ \ddot{y}_2 \end{bmatrix} = \begin{bmatrix} m_1 \\ m_2 \end{bmatrix} g + \begin{bmatrix} -F_l \\ F_l \end{bmatrix} + \begin{bmatrix} -F_a \\ F_a \end{bmatrix} + \begin{bmatrix} -f \\ f \end{bmatrix} - \begin{bmatrix} L \\ 0 \end{bmatrix} - \begin{bmatrix} 0 \\ F_t \end{bmatrix} + \begin{bmatrix} -F_Q \\ F_Q \end{bmatrix}. \tag{23}$$

Damping force

$$\begin{bmatrix} -F_l \\ F_l \end{bmatrix} = \mathrm{sgn}(\dot{y}_1 - \dot{y}_2)\hat{F}_l \begin{bmatrix} -\dot{y}_1 & -\dot{y}_2 \\ \dot{y}_1 & \dot{y}_2 \end{bmatrix} \begin{bmatrix} 1 & -1 \\ -1 & 1 \end{bmatrix} \begin{bmatrix} \dot{y}_1 \\ \dot{y}_2 \end{bmatrix}, \qquad \hat{F}_l = \frac{1}{2}\rho \frac{A^3}{\xi^2 A_0^2}. \tag{24}$$

Spring force

$$\begin{bmatrix} -F_a \\ F_a \end{bmatrix} = \begin{bmatrix} -1 \\ 1 \end{bmatrix} F_a, \quad F_a = p_0 A \left(\frac{1}{1 - (y_1 - y_2/y_0)} \right)^n, \tag{25}$$

Friction force

$$\begin{bmatrix} -f \\ f \end{bmatrix} = \begin{bmatrix} -F_{\mathrm{seal}} \\ F_{\mathrm{seal}} \end{bmatrix} + \begin{bmatrix} -F_{\mathrm{ow}} \\ F_{\mathrm{ow}} \end{bmatrix}, \tag{26}$$

$$\begin{bmatrix} -F_{\mathrm{seal}} \\ F_{\mathrm{seal}} \end{bmatrix} = -k_m \begin{bmatrix} 1 & -1 \\ -1 & 1 \end{bmatrix} \begin{bmatrix} \dot{y}_1 \\ \dot{y}_2 \end{bmatrix} + \mathrm{sgn}(\dot{y}_1 - \dot{y}_2) k_n \begin{bmatrix} -\dot{y}_1 & -\dot{y}_2 \\ \dot{y}_1 & \dot{y}_2 \end{bmatrix} \begin{bmatrix} 1 & -1 \\ -1 & 1 \end{bmatrix} \begin{bmatrix} \dot{y}_1 \\ \dot{y}_2 \end{bmatrix}, \tag{27}$$

$$\begin{bmatrix} -F_{\mathrm{ow}} \\ F_{\mathrm{ow}} \end{bmatrix} = \frac{\mu l}{y_1 - y_2 + B} \left\{ k_t \begin{bmatrix} 0 & -1 \\ 0 & 1 \end{bmatrix} \begin{bmatrix} y_1 \\ y_2 \end{bmatrix} + c_t \begin{bmatrix} 0 & -1 \\ 0 & 1 \end{bmatrix} \begin{bmatrix} \dot{y}_1 \\ \dot{y}_2 \end{bmatrix} + k_t \begin{bmatrix} -1 \\ 1 \end{bmatrix} y_g + c_t \begin{bmatrix} -1 \\ 1 \end{bmatrix} \dot{y}_g \right\}. \tag{28}$$

Ground reaction force

$$\begin{bmatrix} 0 \\ F_t \end{bmatrix} = k_t \begin{bmatrix} 0 & 0 \\ 0 & 1 \end{bmatrix} \begin{bmatrix} y_1 \\ y_2 \end{bmatrix} + c_t \begin{bmatrix} 0 & 0 \\ 0 & 1 \end{bmatrix} \begin{bmatrix} \dot{y}_1 \\ \dot{y}_2 \end{bmatrix} + k_t \begin{bmatrix} 0 \\ 1 \end{bmatrix} y_g + c_t \begin{bmatrix} 0 \\ 1 \end{bmatrix} \dot{y}_g. \tag{29}$$

Active control force

$$\begin{aligned} \begin{bmatrix} -F_Q \\ F_Q \end{bmatrix} = [k_a + \mathrm{sgn}(x)\hat{C}_d k_b x] \Bigg\{ & (\hat{C}_d k_i r + \hat{C}_d k_p \dot{r} + \hat{C}_d k_d \ddot{r}) \begin{bmatrix} -1 \\ 1 \end{bmatrix} \\ & + \hat{C}_d k_i \begin{bmatrix} 1 & -1 \\ -1 & 1 \end{bmatrix} \begin{bmatrix} y_1 \\ y_2 \end{bmatrix} + \hat{C}_d k_p \begin{bmatrix} 1 & -1 \\ -1 & 1 \end{bmatrix} \begin{bmatrix} \dot{y}_1 \\ \dot{y}_2 \end{bmatrix} + \hat{C}_d k_d \begin{bmatrix} 1 & -1 \\ -1 & 1 \end{bmatrix} \begin{bmatrix} \ddot{y}_1 \\ \ddot{y}_2 \end{bmatrix} \Bigg\}. \end{aligned} \tag{30}$$

Displacement of the servo valve

$$x(t) = k_i r(t) + k_p \dot{r}(t) + k_d \ddot{r}(t) + k_i \begin{bmatrix} -1 & 1 \end{bmatrix} \begin{bmatrix} y_1 \\ y_2 \end{bmatrix} + k_p \begin{bmatrix} -1 & 1 \end{bmatrix} \begin{bmatrix} \dot{y}_1 \\ \dot{y}_2 \end{bmatrix} + k_d \begin{bmatrix} -1 & 1 \end{bmatrix} \begin{bmatrix} \ddot{y}_1 \\ \ddot{y}_2 \end{bmatrix}, \tag{31}$$

$$\hat{C}_d = C_d w \sqrt{\frac{1}{\rho}} \sqrt{|p_s - p_l|}. \tag{32}$$

3.2. Static equilibrium solution

To determine the static equilibrium solution of the landing gear system, the time derivatives of the displacements y_1 and y_2, the control force, the ground inputs y_g and $\dot{y}_g$ as well as the lift force L are set to zero. This allows Eq. (23) to reduce to

$$p_0 A \begin{bmatrix} 1 \\ -1 \end{bmatrix} \left(\frac{1}{1 - (y_1 - y_2/y_0)} \right)^n + k_t \left\{ \frac{\mu l}{y_1 - y_2 + B} \begin{bmatrix} 0 & 1 \\ 0 & -1 \end{bmatrix} + \begin{bmatrix} 0 & 0 \\ 0 & 1 \end{bmatrix} \right\} \begin{bmatrix} y_1 \\ y_2 \end{bmatrix} = \begin{bmatrix} m_1 \\ m_2 \end{bmatrix} g. \tag{33}$$

3.3. Dynamic equations around the static equilibrium solution

Let us assume that y_1^*, y_2^* are the solutions of Eq. (33). We define $\tilde{y}_1 = y_1 - y_1^*$ and $\tilde{y}_2 = y_2 - y_2^*$ to represent the solutions of the system relative to its static equilibrium position ($\tilde{y}_1 = 0 - y_2$). This allows representations $y_1 = \tilde{y}_1 - y_1^*$, $y_2 = \tilde{y}_2 + y_2^*$, $\dot{y}_1 = \dot{\tilde{y}}_1$, $\dot{y}_2 = \dot{\tilde{y}}_2$, $\ddot{y}_1 = \ddot{\tilde{y}}_1$, $\ddot{y}_2 = \ddot{\tilde{y}}_2$. Therefore, Eq. (33) becomes

$$\begin{bmatrix} 0 \\ 0 \end{bmatrix} = \begin{bmatrix} m_1 \\ m_2 \end{bmatrix} g + \begin{bmatrix} -F_a^* \\ F_a^* \end{bmatrix} + \begin{bmatrix} -f^* \\ f^* \end{bmatrix} - \begin{bmatrix} L \\ 0 \end{bmatrix} - \begin{bmatrix} 0 \\ F_t^* \end{bmatrix}, \tag{34}$$

which can also be derived from Eq. (23) by using the conditions defining the static solution. The subtraction of Eqs. (34) and (23) yields

$$\begin{bmatrix} m_1 & 0 \\ 0 & m_2 \end{bmatrix} \begin{bmatrix} \ddot{\tilde{y}}_1 \\ \ddot{\tilde{y}}_2 \end{bmatrix} = \begin{bmatrix} -F_a + F_a^* \\ F_a - F_a^* \end{bmatrix} + \begin{bmatrix} -F_l \\ F_l \end{bmatrix} - \begin{bmatrix} 0 \\ F_t - F_t^* \end{bmatrix} + \begin{bmatrix} -f + f^* \\ f - f^* \end{bmatrix} + \begin{bmatrix} -F_Q \\ F_Q \end{bmatrix}. \tag{35}$$

By using Taylor's expansion and neglecting higher-order quantities, the terms arising in Eq. (35) are derived as follows:

Spring force

$$\begin{bmatrix} -F_a + F_a^* \\ F_a - F_a^* \end{bmatrix} = p_0 A^2 n V_0^{-2} [A(n+1)(y_1^* - y_2^*) + V_0] \begin{bmatrix} -1 & 1 \\ 1 & -1 \end{bmatrix} \begin{bmatrix} \tilde{y}_1 \\ \tilde{y}_2 \end{bmatrix}. \tag{36}$$

Damping force

Since the damping force function defined by Eq. (24) is a quadratic function of $\dot{y}_1$ and $\dot{y}_2$ and the function $\mathrm{sgn}(\dot{y}_1 - \dot{y}_2)$ defined by Eq. (13), in their respective Taylor series expansion, both Eq. (24) and its first derivative with respect to $\dot{\tilde{y}}_1 = \dot{y}_1 - \dot{y}_1^* = \dot{y}_1$ and $\dot{\tilde{y}}_2 = \dot{y}_2 - \dot{y}_2^* = \dot{y}_2$ vanish at the equilibrium point $\dot{\tilde{y}}_1 = 0$ and $\dot{\tilde{y}}_2 = 0$, such that

$$\begin{bmatrix} -F_l \\ F_l \end{bmatrix} = 0 \tag{37}$$

and the function $\mathrm{sign}(\dot{\tilde{y}}_1 - \dot{\tilde{y}}_2)$ does not appear in the resultant linearised equation of the system.

Ground reaction force

$$\begin{bmatrix} 0 \\ F_t - F_t^* \end{bmatrix} = k_t \begin{bmatrix} 0 & 0 \\ 0 & 1 \end{bmatrix} \begin{bmatrix} \tilde{y}_1 \\ \tilde{y}_2 \end{bmatrix} + c_t \begin{bmatrix} 0 & 0 \\ 0 & 1 \end{bmatrix} \begin{bmatrix} \dot{\tilde{y}}_1 \\ \dot{\tilde{y}}_2 \end{bmatrix} + k_t \begin{bmatrix} 0 \\ 1 \end{bmatrix} y_g + c_t \begin{bmatrix} 0 \\ 1 \end{bmatrix} \dot{y}_g. \tag{38}$$

Friction force

$$\begin{bmatrix} -f + f^* \\ f - f^* \end{bmatrix} = k_m \begin{bmatrix} -1 & 1 \\ 1 & -1 \end{bmatrix} \begin{bmatrix} \dot{\tilde{y}}_1 \\ \dot{\tilde{y}}_2 \end{bmatrix}. \tag{39}$$

In this model, the offset length l shown in Fig. 3 is assumed negligibly small as used in real designs [8] and therefore the friction force component caused by the offset wheel is not considered. By adopting similar reasoning to the derivation of Eq. (37), we find that the function $\mathrm{sgn}(\dot{\tilde{y}}_1 - \dot{\tilde{y}}_2)$ in Eq. (27) is absent in the linearised equation.

Active control force

$$\begin{aligned} \begin{bmatrix} -F_Q \\ F_Q \end{bmatrix} = {} & [k_a k_x k_i r(t) + k_a k_x k_p \dot{r}(t) + k_a k_x k_d \ddot{r}(t)] \begin{bmatrix} -1 \\ 1 \end{bmatrix} + k_a k_x k_i \begin{bmatrix} 1 & -1 \\ -1 & 1 \end{bmatrix} \begin{bmatrix} y_1^* \\ y_2^* \end{bmatrix} \\ & + k_a k_x k_i \begin{bmatrix} 1 & -1 \\ -1 & 1 \end{bmatrix} \begin{bmatrix} \tilde{y}_1 \\ \tilde{y}_2 \end{bmatrix} + k_a k_x k_p \begin{bmatrix} 1 & -1 \\ -1 & 1 \end{bmatrix} \begin{bmatrix} \dot{\tilde{y}}_1 \\ \dot{\tilde{y}}_2 \end{bmatrix} + k_a k_x k_d \begin{bmatrix} 1 & -1 \\ -1 & 1 \end{bmatrix} \begin{bmatrix} \ddot{\tilde{y}}_1 \\ \ddot{\tilde{y}}_2 \end{bmatrix}. \end{aligned} \tag{40}$$

The substitution of Eqs. (36–40) into Eq. (35) yields

$$\begin{bmatrix} b_1-b_2 & b_2-b_1 \\ b_2-b_1 & b_1-b_2-k_t \end{bmatrix}\begin{bmatrix} \tilde{y}_1 \\ \tilde{y}_2 \end{bmatrix}+\begin{bmatrix} b_3-k_m & k_m-b_3 \\ k_m-b_3 & b_3-k_m-c_t \end{bmatrix}\begin{bmatrix} \dot{\tilde{y}}_1 \\ \dot{\tilde{y}}_2 \end{bmatrix}+\begin{bmatrix} b_4-m_1 & -b_4 \\ -b_4 & b_4-m_2 \end{bmatrix}\begin{bmatrix} \ddot{\tilde{y}}_1 \\ \ddot{\tilde{y}}_2 \end{bmatrix}$$
$$=[b_2r(t)+b_3\dot{r}(t)+b_4\ddot{r}(t)]\begin{bmatrix} 1 \\ -1 \end{bmatrix}+b_2\begin{bmatrix} -1 & 1 \\ 1 & -1 \end{bmatrix}\begin{bmatrix} y_1^* \\ y_2^* \end{bmatrix}+k_t\begin{bmatrix} 0 \\ 1 \end{bmatrix}y_g+c_t\begin{bmatrix} 0 \\ 1 \end{bmatrix}\dot{y}_g, \tag{41}$$

where

$$\begin{aligned} b_1&=p_0A^2nV_0^{-2}[A(n+1)(y_1^*-y_2^*)+V_0],\\ b_2&=k_ak_xk_i,\\ b_3&=k_ak_xk_p,\\ b_4&=k_ak_xk_d. \end{aligned}$$

3.4. Stability condition

The Laplace transform of Eq. (41) gives

$$A\begin{bmatrix} \tilde{y}_1(s) \\ \tilde{y}_2(s) \end{bmatrix}=\begin{bmatrix} b_2+b_3s+b_4s^2 \\ -b_2-b_3s-b_4s^2 \end{bmatrix}r(s)+\begin{bmatrix} 0 \\ k_t+c_ts \end{bmatrix}y_g(s)+b_2\begin{bmatrix} -1 & 1 \\ 1 & -1 \end{bmatrix}\begin{bmatrix} y_1^* \\ y_2^* \end{bmatrix}, \tag{42}$$

where

$$A=\begin{bmatrix} (b_4-m_1)s^2+(b_3-k_m)s+b_1-b_2 & -b_4s^2-(b_3-k_m)s-(b_1-b_2) \\ -b_4s^2-(b_3-k_m)s-(b_1-b_2) & (b_4-m_2)s^2+(b_3-k_m-c_t)s+b_1-b_2-k_t \end{bmatrix}.$$

The characteristic equation of this system is

$$a_0s^4+a_1s^3+a_2s^2+a_3s+a_4=0,$$

where

$$\begin{aligned} a_0&=m_1m_2-(m_1+m_2)b_4,\\ a_1&=(m_1+m_2)(k_m-b_3)+c_t(m_1-b_4),\\ a_2&=(m_1+m_2)(b_2-b_1)+k_t(m_1-b_4)+c_t(k_m-b_3),\\ a_3&=k_t(k_m-b_3)+c_t(b_2-b_1),\\ a_4&=k_t(b_2-b_1). \end{aligned}$$

According to the Routh–Hurwitz stability criterion [27], the necessary and sufficient conditions for stability are

$$\begin{cases} a_0>0, \\ \Delta_1=a_1>0, \\ \Delta_2=\begin{vmatrix} a_1 & a_0 \\ a_3 & a_2 \end{vmatrix}=a_1a_2-a_0a_3>0, \\ \Delta_3=\begin{vmatrix} a_1 & a_0 & 0 \\ a_3 & a_2 & a_1 \\ 0 & a_4 & a_3 \end{vmatrix}=(a_1a_2-a_0a_3)a_3-a_1a_4>0, \\ \Delta_4=a_4>0. \end{cases} \tag{43}$$

A substitution of a_0, a_1, a_2, a_3, a_4 and b_1, b_2, b_3 into Eq. (43) produces the following stability conditions:

$$\begin{cases} k_d < \frac{m_1 m_2}{(m_1+m_2)k_a k_x}, \\ k_p < \frac{c_t m_1^2 + (m_1+m_2)^2 k_m}{k_a k_x (m_1+m_2)^2}, \\ \frac{b_1}{k_a k_x} < k_i < \min[\frac{a_1 a_2 - a_0 k_t (k_m - b_3) + a_0 c_t b_1}{a_0 c_t k_a k_x}, \frac{(a_1 a_2 - a_0 a_3)a_3 + a_1 k_t b_1}{a_1 k_t k_a k_x}], \end{cases} \tag{44}$$

where k_p, k_d and k_i are the adjustable parameters of the controller.

4. Numerical simulation

Based on the analysis described in Sections 2 and 3, and using SIMULINK control system simulation software [17,28–30], numerical simulations of the active landing gear system responses are derived. To illustrate the approach, we investigate an airplane [8] of upper mass 4832.7 kg, lower mass 145.1 kg, lift 7500 N, taxing at 78 m s^{-1} on a runway. For demonstration purpose, Fig. 5 illustrates an assumed half sine-type runway ramp of height 10 cm and length 31.2 m ($= 0.4\,\text{s} \times 78\,\text{m s}^{-1}$) over which the airplane travels. Table 1 presents the parameter values [8] used in this simulation.

4.1. Simulation of stability

As derived from Eq. (44), the parameters defining the stability conditions are given by

$$\begin{cases} k_d < 1.042, \\ k_p < 1.680, \\ 1.23 \times 10^{-5} < k_i < 1.601. \end{cases} \tag{45}$$

The time histories of the vertical dynamic displacement of the centre of gravity of the aircraft relative to the static equilibrium position are shown in Figs. 6–8 as a function of one of the PID control parameters k_p or k_i or k_d, respectively. For each parameter, passive, stable-active, critical stable-active and unstable-active control cases are investigated. As observed in Figs. 6–8, the vertical dynamic displacement illustrates an obvious divergent characteristic if the stability conditions are not satisfied. This provides a measure of confidence in the analysis. Fig. 9 shows an approximate optimum result with control parameters $k_p = 0.6$, $k_i = 0.4$ and $k_d = 0.7$ obtained through numerical calculations. This analysis demonstrates that by choosing suitable active control

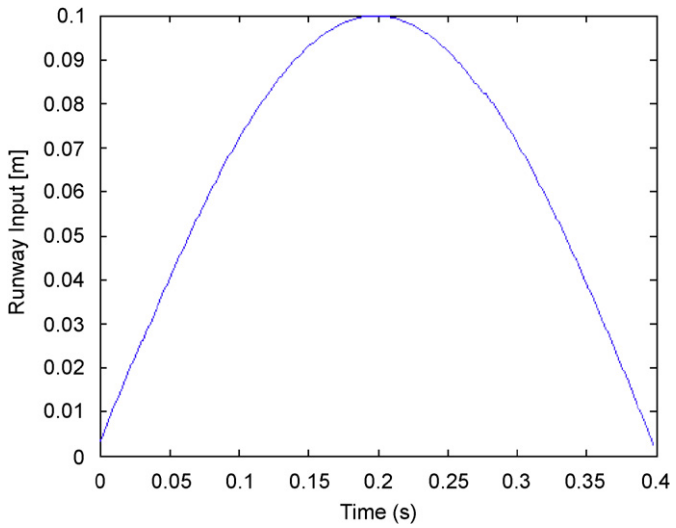

Fig. 5. Runway input excitation modelling a possible ramp on the runway.

Table 1
The values [8] of the parameters used in the simulations

$p_0 = 1.6 \times 10^6$ pa	$A = 1.376 \times 10^{-2}\,\mathrm{m}^2$
$V = 6.88 \times 10^{-3}\,\mathrm{m}^3$	$\rho = 912\,\mathrm{kg\,m}^{-3}$
$g = 9.8\,\mathrm{m\,s}^{-2}$	$A_0 = 6.412 \times 10^{-4}\,\mathrm{m}^2$
$k_t = 1.5 \times 10^6\,\mathrm{N\,m}^{-1}$	$c_t = 2.6 \times 10^6\,\mathrm{N\,s\,m}^{-1}$
$k_m = 0.7 \times 10^4\,\mathrm{N\,s\,m}^{-1}$	$k_n = 0.1 \times 10^5\,\mathrm{N\,s}^2\,\mathrm{m}^{-2}$
$p_{sl} = 0.1 \times 10^6$ pa	$p_{sh} = 20 \times 10^6$ pa
$l = 0.3823\,\mathrm{m}$	$B = 0.05\,\mathrm{m}$
$C_d = 0.1 \times 10^{-5}$	$\mu = 0.01$
$\xi = 0.3$	

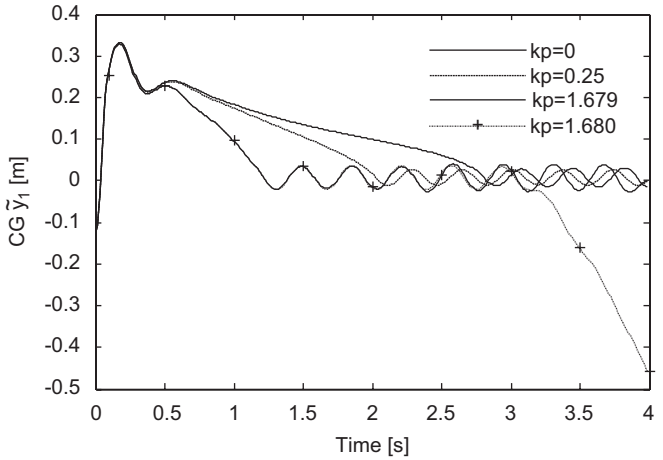

Fig. 6. The influence on the time history of the dynamic displacement $\tilde{y}_1$ of the aircraft's centre of gravity caused by the *velocity or proportional* feedback control parameter k_p. ($k_p = 0$ passive; $k_p = 0.25$ stable-active control; $k_p = 1.679$, critical stable-active control; $k_p = 1.680$, unstable-active control).

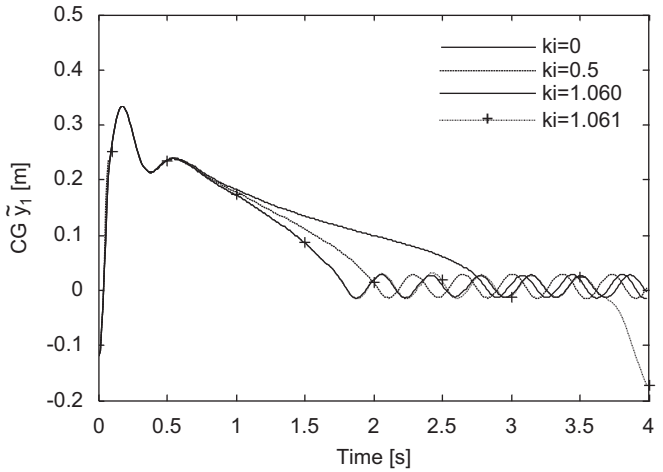

Fig. 7. The influence on the time history of the dynamic displacement $\tilde{y}_1$ of the aircraft's centre of gravity caused by the *displacement or integral* feedback control parameter k_i ($k_i = 0$ passive; $k_i = 0.5$, stable-active control; $k_i = 1.060$, critical stable-active control; $k_i = 1.061$, unstable-active control).

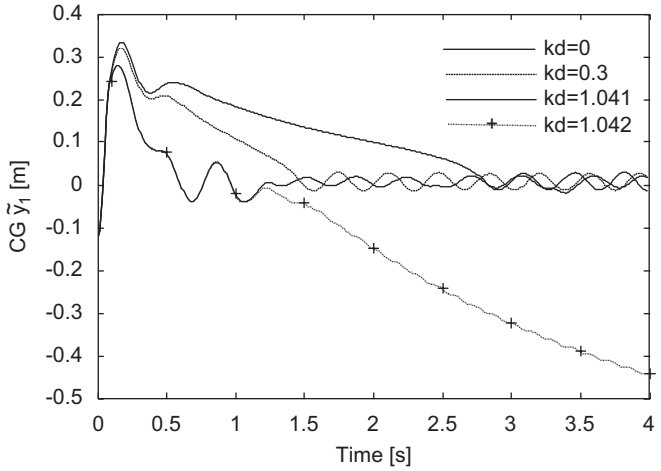

Fig. 8. The influence on the time history of the dynamic displacement $\tilde{y}_1$ of the aircraft's centre of gravity caused by the *acceleration or differential* feedback control parameter k_d ($k_d = 0$, passive; $k_d = 0.3$, stable-active control; $k_d = 1.041$, critical stable-active control; $k_d = 1.042$, unstable-active control).

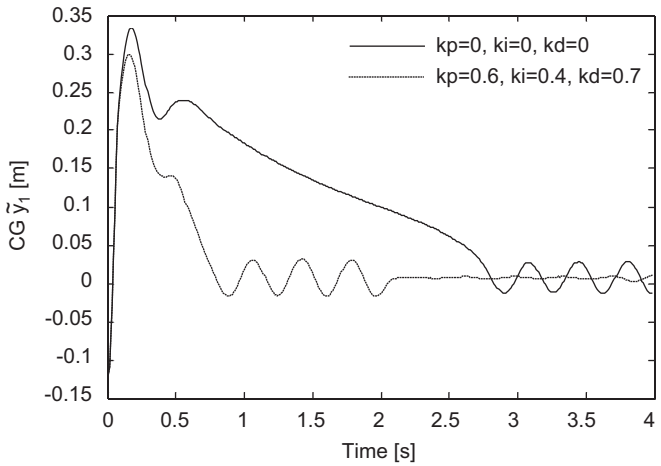

Fig. 9. The time history of the dynamic displacement $\tilde{y}_1$ of the aircraft's centre of gravity for the active landing gear system with control parameter values $k_p = 0.6$, $k_i = 0.4$, $k_d = 0.7$, which represent an approximate optimum selection.

parameter values, an effective reduction of the peak value of the dynamic displacement caused by runway excitations is achieved.

4.2. Simulation of performance

The vertical displacement of the centre of gravity of the aircraft is an important parameter in designing an aircraft landing gear system [1]. It involves the sensitivity of the designed system to unevenness of the runway surface. It is expected that an aircraft rapidly returns to its original equilibrium state when influenced by a runway excitation. This objective was realised in an effective manner by introducing an active controller. For example, through numerical simulation experiments adopting a wide range of control parameters, we found that the approximate optimum set $k_p = 0.6$, $k_i = 0.4$ and $k_d = 0.7$ produced the best control efficiency as shown in Fig. 9. This set of control parameters corresponds to a transfer function of the controller given by

$$k(s) = 0.6 + \frac{0.4}{s} + 0.7s. \tag{46}$$

As shown in Fig. 9, the passive system requires approximately 2.8 s for the aircraft to return to its static equilibrium position. This time is reduced to approximately 0.8 s using this active system, and demonstrates a significant improvement over the performance of the passive system. Figs. 10–14 show a detailed comparison of the performance of the two systems. For example, for the active system, Fig. 10 shows that in the first 0.4 s there is a 13% decrease of the aircraft's displacement response, making taxiing smoother and therefore the crew/passenger comfort improved.

The amplitude of the impact force transmitted to the airframe affects the structural strength and the fatigue life of the aircraft [11,12]. Figs. 11 and 12 show that both the spring and damping forces are reduced using the active system. Fig. 13 indicates that there is a 12% decrease of the transmitted force in the passive landing gear if the active control is used.

Fig. 14 illustrates the time history of the servo-valve displacement relative to the active control force as shown in Fig. 15. It can be seen that for a positive strut stroke, the servo valve is opened positively and the oil is drawn into the landing gear from the active control system producing a positive active control force. In the reverse case, for a negative strut stroke, the servo valve is opened in a negative manner, causing the oil to flow

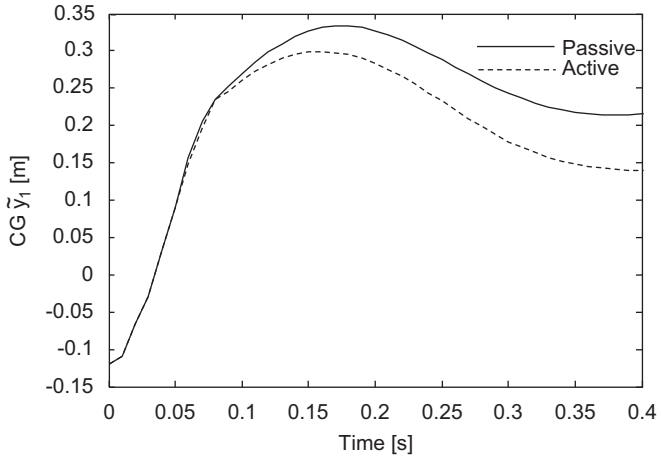

Fig. 10. The time histories of the displacement $\tilde{y}_1$ of the aircraft's centre of gravity when passive and optimum active landing gear systems are used.

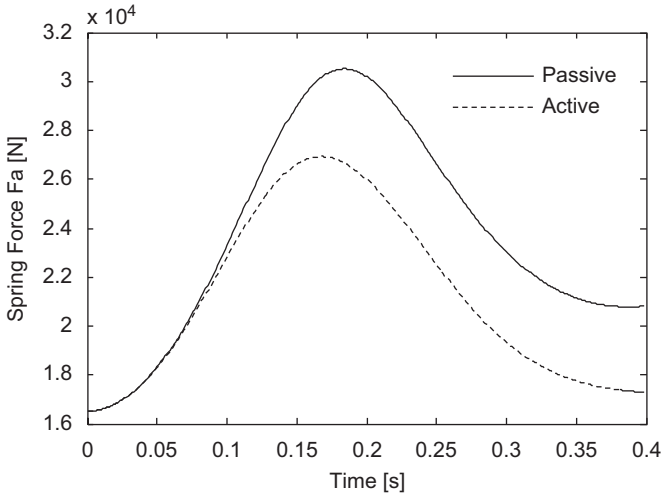

Fig. 11. The spring force time histories for the passive and optimum active landing gear systems.

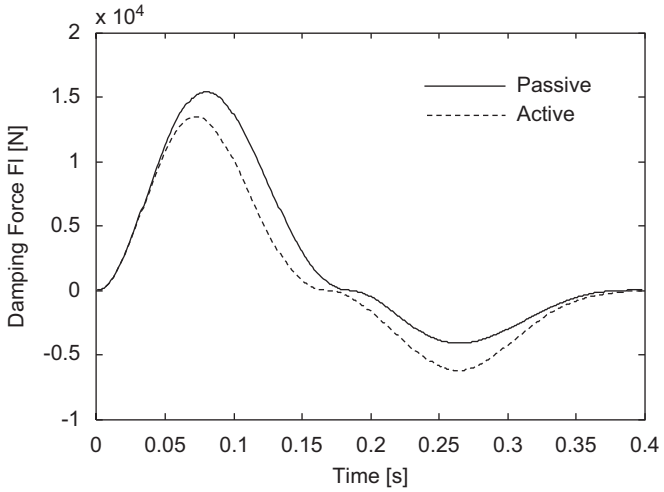

Fig. 12. The damping force time histories for the passive and optimum active landing gear systems.

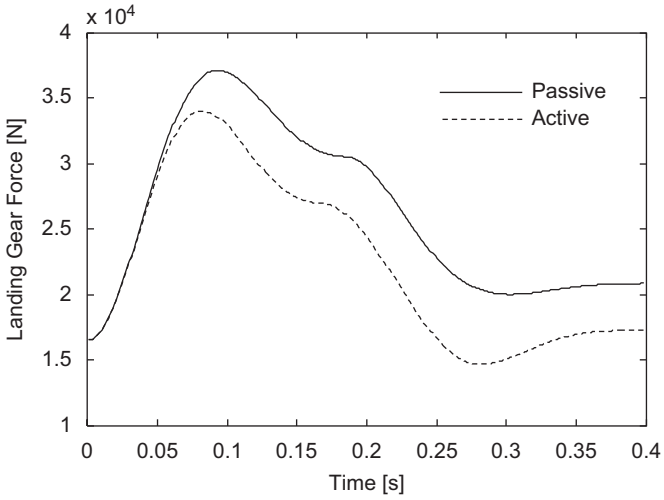

Fig. 13. The impact forces of the passive and optimum active landing gear systems.

out of the landing gear from the active control system creating a negative active control force. Such behaviour reduces the vibration magnitude and time external environmental conditions exert on the aircraft and results in improvements to the longevity of the airframe and comfort to passengers.

5. *Conclusion and discussion*

Through the development of a proposed mathematical model and stability analysis, this investigation describes and discusses the behaviour characteristics of an active landing gear system. Numerical simulation experiments demonstrate the suitability of the mathematical model and, through calculated data, an analysis of an active landing gear design. Comparisons of passive and active systems identify the effectiveness of the latter through significant reduction in the magnitude of the displacement of the centre of gravity of the aircraft and the loads transmitted to the airframe by the landing gear during aircraft landing and taxiing. It is further demonstrated that by using an active landing gear system, a reduction in the time length of responses to return to their static equilibrium positions is achieved, thus improving the performance of the landing gear, the

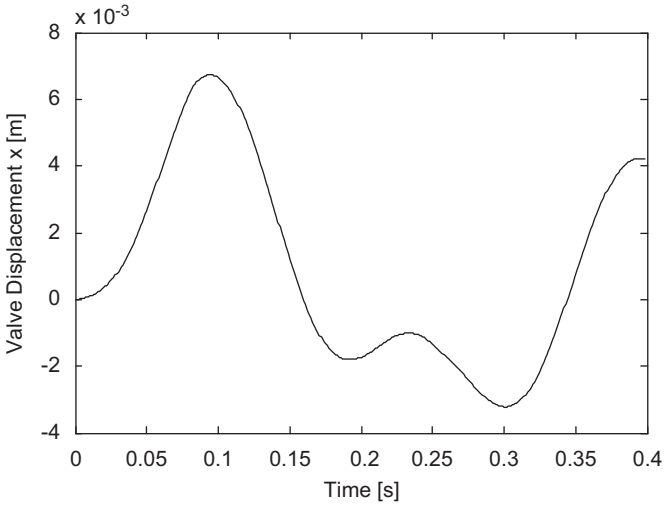

Fig. 14. The dynamic response of the servo-valve displacement.

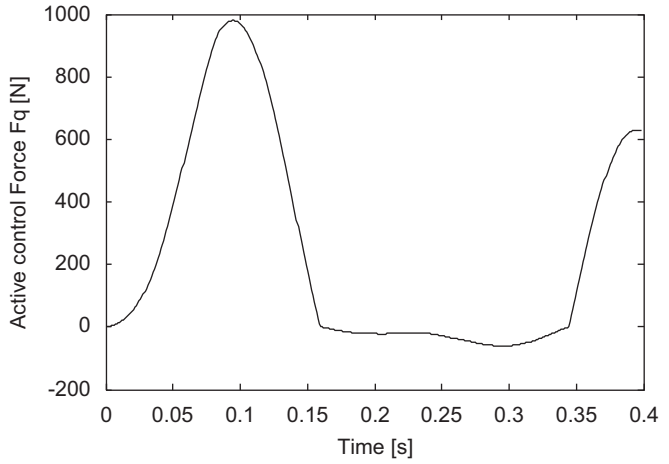

Fig. 15. The active control force produced by the optimum active landing system.

fatigue life of the airframe and landing system, crew and passenger comfort, the pilot's ability to control the plane during ground operations, etc. and a reduction of the influence of runway unevenness.

This study provides a theoretical and numerical approach to initiate the design of a realisable active landing gear system, but significant obstacles must be solved before introduction. For example, power supply, space limitations, structural and environmental problems, safety considerations requiring full understanding of the nonlinear system's behaviour and stability, etc. Whilst the linearised equations are used here to study the asymptotic stability of a nonlinear system about an equilibrium point, the deviation from linearity is assumed small, but if an accurate analysis is required, then recourse to the analysis of a nonlinear system is required.

References

[1] N.S. Currey, Aircraft landing gear design: principles and practices, *AIAA Education Series, AIAA* (1998).
[2] R. Freymann, Actively damped landing gear system, Landing Gear Design Loads Conference No. 20, AGARD CP-484, 1991.
[3] R. Freymann, An experimental–analytical routine for the dynamic qualification of aircraft operating on rough runway surfaces, *AGARD R-731* (1987).

[4] T. Catt, D. Cowling, A. Shepherd, Active landing gear control for improved ride quality during ground roll, SDL Report No. 232, Stirling Dynamics Limited, 1992.
[5] T.W. Lee, Dynamic response of landing gears on rough repaired runway, *Menasco Aero Systems Division* (1998) 124–135.
[6] I. Ross, R. Edson, Application of active control landing gear technology to the A-10 aircraft, *NASA CR-166104* (1983).
[7] W.E. Howell, J.R. Mc Gehee, R.H. Daugherty, W.A. Vogler, F-106B airplane active control landing gear drop test performance, Landing Gear Design Loads Conference No. 21, AGARD CP-484, 1991.
[8] C.H. Lucas, Modeling and validation of a navy A6-intruder actively controlled landing gear system, *NASA TP-209124* (1999).
[9] I. Ross, R. Edson, An electronic control for an electro-hydraulic active control landing gear for the F-4 aircraft, *NASA CR-3552* (1982).
[10] I.P. Jocelyn, An overview of landing gear dynamics, *NASA TM-209143* (1999).
[11] B.W. Payne, A.E. Dudman, B.R. Morris, M. Hockenhull, Aircraft dynamic response to damaged and repaired runways, *AGARD CP-326* (1982).
[12] Y.H. Jia, Taxiing performance analysis of active control of landing gear, *Acta Aeronautica et Astronautica Sinica* 20 (6) (1999) 545–548.
[13] G.L. Ghiringhelli, Testing of semiactive landing gear control for a general aviation aircraft, *Journal of Aircraft* 37 (4) (2000) 607–616.
[14] D. Karnopp, Active damping in road vehicle suspension system, *Vehicle Systems Dynamics* 12 (6) (1983) 291–316.
[15] R.M. Goodall, Active controls in ground transportation—a review of the state-of-the-art and future potential, *Vehicle Systems Dynamics* 12 (4) (1983) 225–257.
[16] J.K. Hedrick, The application of active and passive suspension techniques to improve vehicle performance, Final Report, US Department of Transportation, Contract DTRS5680-C-00018, 1983.
[17] SIMULINK—dynamic system simulation for MATLAB, version 2—using SIMULINK, The Math Works Inc., 1997.
[18] D.L. Xu, Y.R. Li, Mathematical model research on aircraft landing gear, *Journal of System Simulation* 17 (4) (2005) 831–833.
[19] P. Jin, H. Nie, Dynamic simulation model and parameter optimization for landing gear impact, *Journal of Nanjing University of Aeronautics & Astronautics* 35 (5) (2003) 498–502.
[20] J.J. Sharp, *BASIC Fluid Mechanics*, Butterworths, London, 1988.
[21] E. Bakker, H.B. Pacejka, L. Linder, New tire model with an application in vehicle dynamic studies, *Progress in Technology* 57 (1995) 439–452.
[22] A. Datta, M.T. Ho, S.P. Bhattacharyya, *Structure and Synthesis of PID Controllers*, Springer, London, 2000.
[23] S.M. Shinners, *Control System Design*, Wiley, New York, 1964.
[24] C.R. Fuller, S.J. Elliott, P.A. Nelson, *Active Control of Vibration*, Academic Press, San Diego, 1996.
[25] J.T. Xing, Y.P. Xiong, W.G. Price, Passive–active vibration isolation systems to produce zero or infinite dynamic modulus: theoretical and conceptual design strategies, *Journal of Sound and Vibration* 286 (2005) 615–636.
[26] C. Chicone, *Ordinary Differential Equations with Applications*, second ed., Springer, New York, 2006.
[27] A. Hurwitz, On the condition under which an equation has only roots with negative real part, in: R. Bellman, R. Kalaba (Eds.), *Selected Papers on Mathematical Trends in Control Theory*, Dover, New York, 1964, pp. 72–82.
[28] S. Wolfram, *The Mathematica Book*, Wolfram Media/Cambridge University Press, New York, 1996.
[29] A. Shepherd, T. Catt, D. Cowling, An aircraft landing gear simulation parametric leg model, SDL Report No. 234, Stirling Dynamics Limited, 1993.
[30] J.N. Daniels, A method for landing gear modeling and simulation with experimental validation, *NASA CR-201601* (1996).